pubs.acs.org/accounts

ACCOUNTS of chemical research

SPECIAL ISSUE, 2018

THE INTERFACE OF BIOLOGY WITH NANOSCIENCE AND ELECTRONICS

ACS Publications
Most Trusted. Most Cited. Most Read.

www.acs.org

ACCOUNTS of chemical research

Article

Cite This: Acc. Chem. Res. 2018, 51, 309–318

pubs.acs.org/accounts

Mesh Nanoelectronics: Seamless Integration of Electronics with Tissues

Published as part of the Accounts of Chemical Research special issue "The Interface of Biology with Nanoscience and Electronics".

Xiaochuan Dai,[†] Guosong Hong,[†] Teng Gao,[†] and Charles M. Lieber*[,†,‡]

[†]Department of Chemistry and Chemical Biology and [‡]Harvard John A. Paulson School of Engineering and Applied Sciences, Harvard University, Cambridge, Massachusetts 02138, United States

CONSPECTUS: Nanobioelectronics represents a rapidly developing field with broad-ranging opportunities in fundamental biological sciences, biotechnology, and medicine. Despite this potential, seamless integration of electronics has been difficult due to fundamental mismatches, including size and mechanical properties, between the elements of the electronic and living biological systems.

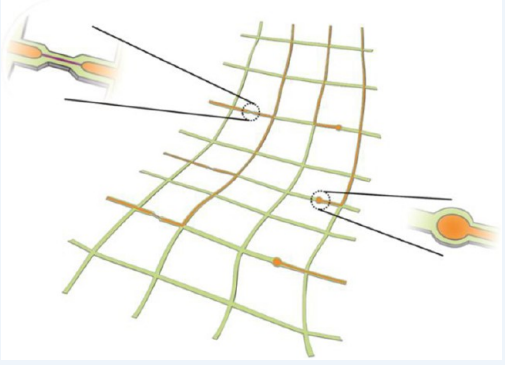

In this Account, we discuss the concept, development, key demonstrations, and future opportunities of mesh nanoelectronics as a general paradigm for seamless integration of electronics within synthetic tissues and live animals. We first describe the design and realization of hybrid synthetic tissues that are innervated in three dimensions (3D) with mesh nanoelectronics where the mesh serves as both as a tissue scaffold and as a platform of addressable electronic devices for monitoring and manipulating tissue behavior. Specific examples of tissue/nanoelectronic mesh hybrids highlighted include 3D neural tissue, cardiac patches, and vascular constructs, where the nanoelectronic devices have been used to carry out real-time 3D recording of electrophysiological and chemical signals in the tissues. This novel platform was also exploited for time-dependent 3D spatiotemporal mapping of cardiac tissue action potentials during cell culture and tissue maturation as well as in response to injection of pharmacological agents. The extension to simultaneous real-time monitoring and active control of tissue behavior is further discussed for multifunctional mesh nanoelectronics incorporating both recording and stimulation devices, providing the unique capability of bidirectional interfaces to cardiac tissue.

In the case of live animals, new challenges must be addressed, including minimally invasive implantation, absence of deleterious chronic tissue response, and long-term capability for monitoring and modulating tissue activity. We discuss each of these topics in the context of implantation of mesh nanoelectronics into rodent brains. First, we describe the design of ultraflexible mesh nanoelectronics with size features and mechanical properties similar to brain tissue and a novel syringe-injection methodology that allows the mesh nanoelectronics to be precisely delivered to targeted brain regions in a minimally invasive manner. Next, we discuss time-dependent histology studies showing seamless and stable integration of mesh nanoelectronics within brain tissue on at least one year scales without evidence of chronic immune response or glial scarring characteristic of conventional implants. Third, armed with facile input/output interfaces, we describe multiplexed single-unit recordings that demonstrate stable tracking of the same individual neurons and local neural circuits for at least 8 months, long-term monitoring and stimulation of the same groups of neurons, and following changes in individual neuron activity during brain aging.

Moving forward, we foresee substantial opportunities for (1) continued development of mesh nanoelectronics through, for example, broadening nanodevice signal detection modalities and taking advantage of tissue-like properties for selective cell targeting and (2) exploiting the unique capabilities of mesh nanoelectronics for tackling critical scientific and medical challenges such as understanding and potentially ameliorating cell and circuit level changes associated with natural and pathological aging, as well as using mesh nanoelectronics as active tissue scaffolds for regenerative medicine and as neuroprosthetics for monitoring and treating neurological diseases.

BACKGROUND AND MOTIVATION

Bioelectronics involves the union of electronics with biological systems such that the electronics can monitor or modulate properties of the system or both.[1−4] The field has a long history, from Galvani's 1780s studies of exciting frog muscles[3] to current medical devices, including implanted cardiac pacemakers and deep brain stimulators.[4] Remarkably, these latter medical devices have many of the same bioelectronic interface features as in Galvani's experiments, comparatively

Received: October 31, 2017
Published: January 30, 2018

DOI: 10.1021/acs.accounts.7b00547
Acc. Chem. Res. 2018, 51, 309–318

rigid metal electrode surfaces in contact with soft tissues. For example, implantable microwires and silicon-based neural probes with microscale metal devices have allowed recording of brain activity with single neuron level spatiotemporal resolution in live animals and even human subjects.[4] Yet, the large mismatch in stiffness between these probes and brain tissue results in relative shear motion, glial scar formation, and neuron depletion at the probe−brain interfaces[5] that prevent long-term tracking of the same neurons and their encompassing neural circuits. In essence, the bioelectronic devices have very little similarity to the biological system they are designed to monitor.

One approach we initiated over a decade ago to bridge the gap between electronic and biological systems centered on incorporating nanoscale devices to enable individual elements to interface at the subcellular level as occurs naturally in biology.[6,7] For example, we introduced two-dimensional (2D) chip-based arrays of nanowire field-effect-transistors (FETs) capable of mapping highly localized action potentials (APs) from cultured neurons and acute brain slices with subcellular resolution,[7,8] showing the capability to record both APs from the localized synapse-like junctions formed by neurites crossing individual nanowire FETs[7] and localized excitatory postsynaptic potential[8] not possible with conventional metal microelectrodes.

Recognizing the limitation of planar electronics for interfacing with three-dimensional (3D) biological systems also led us, through the deep understanding and synthetic versatility of nanowires,[2,3] to develop the first 3D nanowire FET nanoprobes.[9] These 3D nanoprobes were enabled by introducing two *cis*-topological kinks or stereocenters during nanowire growth to localize an active FET at the tip of an acute-angle kinked silicon nanowire.[9] This approach allowed for localization of a point-like detector away from the microscale electrical contacts and, following surface functionalization with phospholipid bilayers, yielded cellular internalization and intracellular recording with minimal external forces using both substrate-based and fully free-standing 3D kinked nanowire probes.[9,10] These studies have demonstrated how advances in nanoelectronics enabled by synthesized nanowire devices allow for interfacing at scales more relevant to biology, yet the presentation of these arrays of devices on relatively rigid substrates[6−9] or as individual probes[10] has precluded 3D seamless integration of bioelectronic systems with synthetic and natural tissues.

To overcome this major limitation that has persisted in the field since Galvani's work,[3] we have focused on development of a new paradigm for bioelectronics, tissue-like electronics, in which we create 3D networks of addressable devices where all elements of the network have cellular or subcellular dimensions, the network mechanical properties are similar to the tissue, and the network structure allows both 3D interpenetration of cells and diffusion of biochemical species (Figure 1).[2,3,11−15] Below we describe the implementation of this paradigm within the context of seamless 3D integration of nanoelectronics with synthetic tissues and live animals, including unique capabilities for stable 3D monitoring and modulation of cellular or tissue activity relevant to areas from pharmacological screening in cardiac tissue patches to single neuron level changes associated with aging, and then conclude a discussion of where we foresee substantial future opportunities in fundamental research through electronic therapeutics.

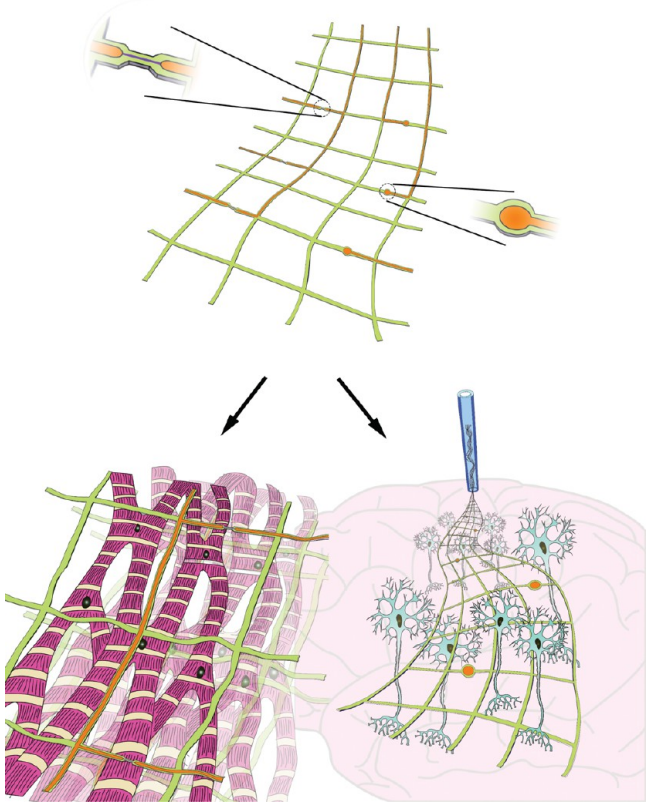

Figure 1. Seamless integration of mesh nanoelectronics with synthetic tissues and live animals. Mesh nanoelectronics with devices (top) can serve as active scaffolds for synthetic tissues (bottom left) or be delivered into live animals for integration and interrogation of neural tissue (bottom right).

MESH NANOELECTRONICS

Our paradigm for tissue-like electronics consisting of a macroporous mesh structure with addressable electronic devices (Figure 1), hereafter termed mesh nanoelectronics, was first realized in terms of the analogous biological functional elements across nanometer-to-centimeter size scales.[11] At the individual device level, it is possible to incorporate semiconductor nanowires with rationally defined properties[2,3,6−10] as subcellular size active sensors or metal microelectrodes as cellular size passive sensors or larger-scale stimulators.[12−15] At the network level, the macroporous mesh structure with addressable devices is readily fabricated by standard lithography methods on a 2D substrate first coated with a release layer. In this process, we use an organic resist, which is converted to a biocompatible polymer during lithography processing, both as the key structural material for the mesh and as the material embedding and passivating the ultrathin metal interconnects, while leaving the nanowire or metal devices exposed. Following fabrication and release from the substrate, the mesh nanoelectronics can be transformed into different 3D topologies and seeded with cells to yield electronically innervated synthetic tissues (Figure 1, bottom left) or loaded into a syringe needle and injected into the brain or other tissue regions of live animals in a minimally invasive manner (Figure 1, bottom right).

This general strategy allows facile tailoring of all key elements and the properties of the mesh nanoelectronics. For example, the device type, spatial configuration, and number are readily defined in a deterministic manner by a combination of

DOI: 10.1021/acs.accounts.7b00547
Acc. Chem. Res. 2018, 51, 309−318

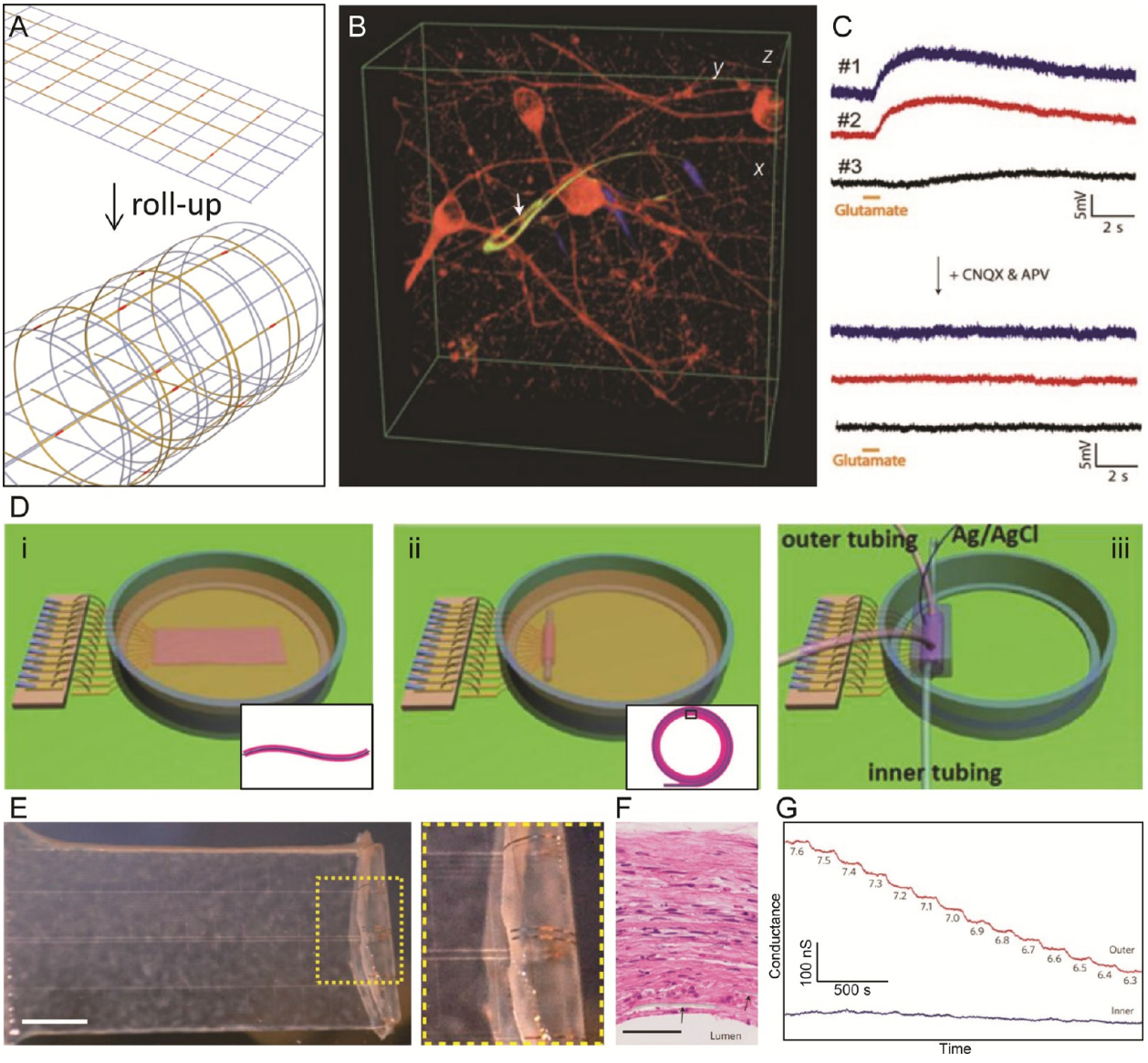

Figure 2. Mesh nanoelectronics: innervated synthetic tissues. (A) Schematic of 2D mesh nanoelectronics (as fabricated) that is rolled up into 3D scaffolds; red dots indicate positions of addressable devices. (B) 3D reconstructed confocal fluorescence image of rat hippocampal neurons (red) cultured for 2 weeks in mesh nanoelectronics (yellow). Dimensions x = 127 μm; y = 127 μm; z = 68 μm. (C) Multiplexed electrical recording of local field potential following glutamate addition (orange segments) without (top) and with (bottom) synaptic blockers. (D) Schematics of mesh nanoelectronics scaffold seeded with HASMCs (i), rolled into tubular structure (ii), and connected to tubing and PDMS chamber for endovascular and extravascular perfusion (iii). (E) Photographs of a single HASMC sheet cultured on mesh nanoelectronics scaffold (left) and enlarged view (right) of dashed region. Scale bar, 5 mm. (F) Hematoxylin and eosin stained section cut perpendicular to the tube axis. Small black arrows mark positions of two mesh elements. Scale bar, 50 μm. (G) Changes in conductance over time from two nanowire FETs located in the outermost (red) and innermost (blue) layers of a mesh nanoelectronics-innervated blood vessel, where pH is varied in the outer tubing and fixed in the inner tubing. Reproduced with permission from ref 11. Copyright 2012 Nature Publishing Group.

assembly[16,17] and lithography to meet specific design goals for experiments. In addition, the structural design of the mesh nanoelectronics, including the width, thickness, and unit cell of the polymer elements, is used to control the mechanical properties such that they are comparable to those of tissues being targeted,[12−14] as well as allow for 3D interpenetration of different cell types and diffusion of important biochemical species. Below we first focus on the studies of mesh nanoelectronics for 3D innervation of synthetic tissues[11,12] and then make a conceptual jump forward with seamless 3D integration within the brain.[13−15,18−20]

MESH NANOELECTRONICS IN SYNTHETIC TISSUES

A diverse variety of mesh nanoelectronics/synthetic tissue hybrid materials with interpenetrating 3D networks of addressable devices and cells have been prepared by the following general procedures.[11,12,21] First, the substrate portion of the mesh nanoelectronics is transformed from planar as-fabricated structure to a specific 3D configuration by exploiting either built-in strain for self-organization or mechanical deformations such as folding or rolling-up (Figure 2A). The mesh nanoelectronics structure is either seeded with specific cell types directly or first combined with a conventional passive biomaterial scaffold, such as collagen, alginate, or PLGA, before

DOI: 10.1021/acs.accounts.7b00547
Acc. Chem. Res. 2018, 51, 309−318

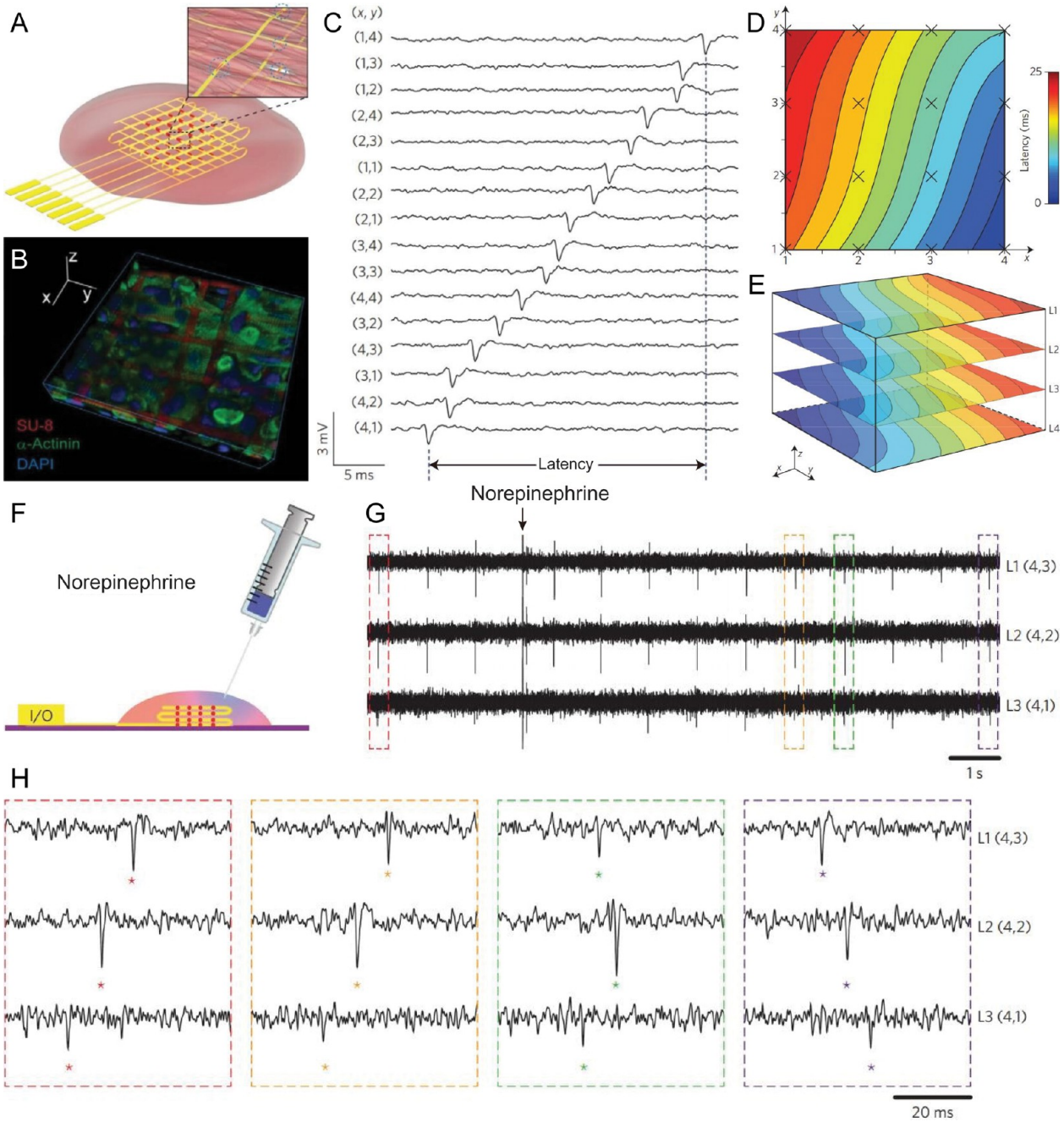

Figure 3. 3D mapping of APs in mesh nanoelectronics-innervated cardiac tissue. (A) Schematic illustrating the hybrid synthetic tissue formed by culturing cardiomyocytes in folded 3D mesh nanoelectronics with red dots indicating silicon nanowire FETs. (B) Reconstructed 3D confocal fluorescence image of mesh nanoelectronics-innervated cardiac tissue. Scale bars, 25 μm. (C) Simultaneous traces recorded from 16 sensors in the top layer (L1). (D) Isochronal map of time latency in L1. Mapping area, ~25 mm^2. (E) 3D isochronal latency maps from L1 to L4 for the 3D cardiac tissue. Mapping area, ~25 mm × 25 mm × 200 μm. (F) Schematic of the focal injection of norepinephrine. (G) Time-dependent traces from three sensors in L1, L2, and L3 with synchronized and periodic APs. The blue arrow indicates the injection of ~25 μL of norepinephrine at a concentration of 100 μM. (H) Enlarged traces of the four dashed boxes in part G, highlighting the time latency variation at different times relative to addition of norepinephrine. Reproduced with permission from ref 12. Copyright 2016 Nature Publishing Group.

cell seeding. Finally, the mesh nanoelectronics hybrid with cells is cultured to fully develop the 3D innervated tissues, where measurements can be carried out both during tissue maturation and in a fully developed state.

For example, embryonic rat hippocampal neurons were cultured in a rolled-up mesh nanoelectronics hybrid with silicon nanowire FETs to yield 3D innervated neural tissues.[11] Notably, the 3D confocal micrograph (Figure 2B) of the hybrid recorded following 2-week culture showed clearly seamless interpenetration of the neural network and similar feature size mesh nanoelectronics, with individual neurites often passing through the ring structures supporting individual nanowire FETs. This intimate nanoelectronic/neural interface further allowed for multiplexed 3D recording of local field potential (LFP) activity induced by addition of glutamate and subsequent suppression of activity by synaptic blockers (Figure 2C).[11]

DOI: 10.1021/acs.accounts.7b00547
Acc. Chem. Res. 2018, 51, 309−318

A second example and one that follows directly from the roll-up concept is the development of innervated vascular tissue constructs.[11] Schematics and experimental demonstrations of this concept (Figure 2D,E) show human aortic smooth muscle cells (HASMCs) initially cultured on 2D mesh nanoelectronics (Figure 2D(i),E) to develop an intimate mesh nanoelectronics—HASMCs interface, followed by rolling into multilayer 3D tubular structures and further culture to yield matured vascular constructs without macroscopic delamination or desquamation (Figure 2D(ii),E). Cross-sectional images of the stained innervated vascular construct (Figure 2F) revealed tight integration of elongated cells, collagenous nanofibers, and embedded mesh nanoelectronics. These hybrid constructs with chemical sensing capabilities of the nanowire FETs[6] were used as a platform to monitor pH through the tissue as the endovascular and extravascular pH was varied (Figure 2D(iii)). Notably, as the extravascular pH was varied stepwise with luminal pH fixed, nanowire FETs in the outermost layer tracked this pH change, while the devices in the innermost layer showed minor baseline fluctuations (Figure 2G). These mesh nanoelectronics-innervated vascular constructs thus demonstrate capability as biomedical devices to study inflammation, ischemia, tumor microenvironments, or other forms of metabolic acidosis.[22,23]

A third example where mesh nanoelectronics/synthetic tissues have been examined in considerable detail centers on innervated cardiac tissue patches.[12] For example, neonatal rat ventricular cells seeded in mesh nanoelectronics/PLGA hybrid scaffolds can be readily "folded" to yield 3D innervated structures (Figure 3A) with multiple layers of addressable nanoelectronic devices for monitoring and modulating tissue behavior.[12] A 3D confocal fluorescence image of a typical hybrid following 7 days of culture (Figure 3B) reveals a high density of cardiomyocytes in close contact with and aligned to the mesh nanoelectronics. Extended 2−3 week time scale studies showed little effect of the mesh nanoelectronics on the cell viability, thus demonstrating long-term biocompatibility. Additionally, multiplexed recording of extracellular cardiac APs (Figure 3C) demonstrate single-shot sub-millisecond resolution, which has been exploited to map the time latency between signals from one (Figure 3D) or multiple device layers (Figure 3E) associated with AP propagation across the 3D tissue.

This 3D mapping capability has been exploited to explore several areas in unique ways including tissue development, arrhythmia disease models and closed-loop electronic therapeutics.[12] First, 3D real-time mapping of APs carried out at 2, 4, 6, and 8 days *in vitro* revealed expansion of spontaneous beating regions with volume percentage of detectable activity increasing from ca. 50% to 98% over this period. The unique capability to directly map 3D functional network provides an advanced method to study tissue engineering and regeneration, including studies of stem cell differentiation, growth factors, and ischemia. In addition, focal injection of norepinephrine, a β-adrenergic receptor agonist, was used as an model system to induce arrhythmia.[24] Following injection at one position of an innervated cardiac tissue (Figure 3F), simultaneous real-time recording of APs in 3D (Figure 3G) yielded clear evidence for arrhythmia and subsequent tissue self-adaptation with millisecond resolution. Representative data from three nanowire FET sensors in different layers before and after norepinephrine injection (Figure 3G,H) highlighted the dynamic instability of the conduction pathway, where the AP initially propagated from sensor L3(4,1) to L1(4,3) before the injection, followed by an earlier depolarization around sensor L1(4,3) leading to reversal of the propagation direction 5−10 s postinjection. These critical spatiotemporal variations associated with norepinephrine and other drugs[11,12] would be difficult to detect using methods that require scanning and averaging of APs in 3D[25] and highlight one of the clear advantages of our mesh nanoelectronics 3D innervated tissues as models for pharmacological screening in the future.

Finally, we have also investigated cardiac tissues innervated with multifunctional mesh nanoelectronics incorporating both sensor and stimulator devices as a step toward closed-loop nanoelectronics−tissue hybrids as implants (Figure 4A).[12]

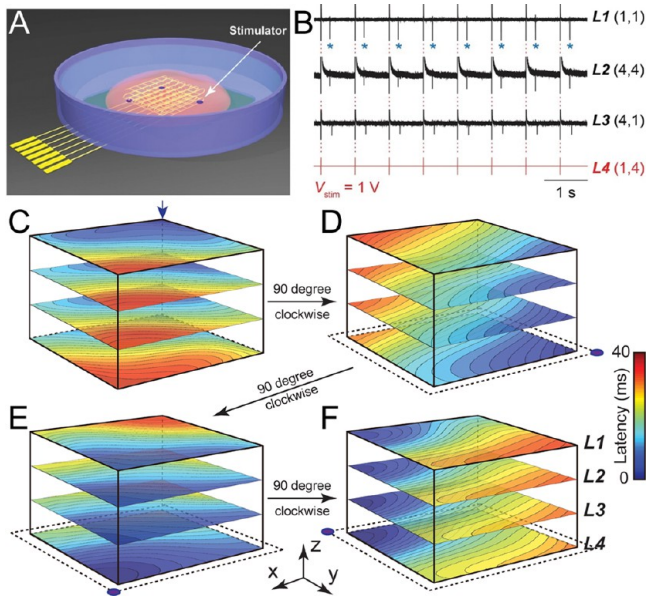

Figure 4. Simultaneous recording and modulation of APs in mesh nanoelectronics-innervated cardiac tissue. (A) Schematic illustrating the positions of individually addressable stimulators (purple dots) in the 3D mesh nanoelectronics. (B) Time-dependent traces recorded from nanowire FETs in layers L1, L2, and L3 under a periodic biphasic stimulation spike train in L4. Blue asterisks highlight APs (downward spikes) versus capacitive coupling peaks (red dashed lines). (C−F) 3D isochronal time latency maps showing the original pacemaker foci location (blue arrow), and sequential 90° clockwise rotations of the AP propagation direction induced by the indicated simulators (purple dots in lower corners). Reproduced with permission from ref 12. Copyright 2016 Nature Publishing Group.

Significantly, application of a stimulation spike train (1 V, 1.25 Hz) in the mesh nanoelectronics-innervated cardiac tissue (Figure 4B) locked the AP peaks recorded in different regions of the tissue to the stimulation. Moreover, with the same conditions it is possible to control precisely AP propagation direction; that is, sequential stimulation at different corners of the hybrid tissue rotated the AP propagation directions by 90° at each step (Figure 4C−F).[12] These results provide a proof-of-concept for closed-loop control of implanted cardiac patches that would allow for precise monitoring and modulation of cardiac electrophysiology postsurgery, a critical capability not currently possible with conventional stimulators.[26]

MESH NANOELECTRONICS IN LIVE ANIMALS

Moving from mesh nanoelectronics/synthetic tissue hybrids to innervating tissue in live animals requires several hurdles to be addressed. First, a minimally invasive method that affords

DOI: 10.1021/acs.accounts.7b00547
Acc. Chem. Res. 2018, 51, 309−318

precise targeting of specific tissue regions is needed to implant the mesh nanoelectronics. Second, the responses of the tissue and cells to the mesh nanoelectronics must be characterized; that is, whether it elicits an immune response. Third, an input/output (I/O) instrument interface compatible with minimally invasive delivery and *in vivo* measurements is needed to explore the potentially unique characteristics of the tissue-like electronics. We discuss each of these key points within the context of implanting the mesh nanoelectronics into the brains of live rodents.

To solve the challenge of minimally invasive delivery, we proposed and demonstrated a unique solution whereby the mesh nanoelectronics is treated as a "biological reagent" that is delivered to the tissue by syringe injection (Figure 5).[13,18] The

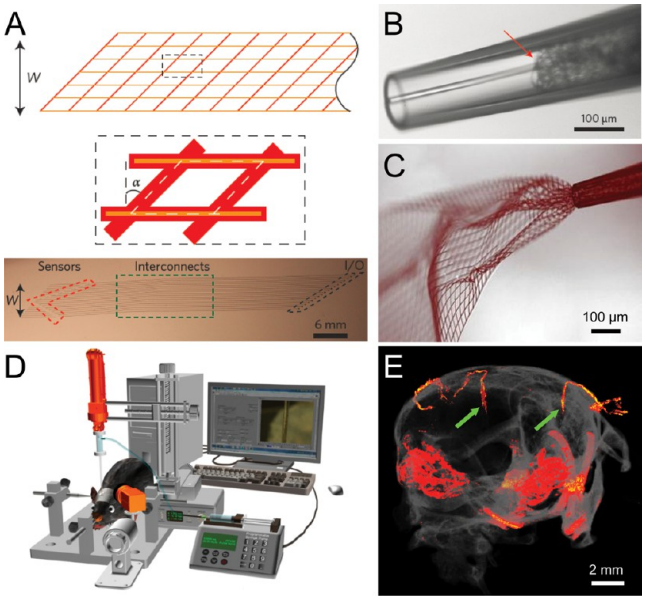

Figure 5. Syringe-injection of mesh nanoelectronics into live animals. (A) Schematic of syringe-injectable mesh nanoelectronics. Orange and red lines represent polymer-encapsulated metal interconnects and supporting polymer elements, respectively. The dashed boxes (bottom) highlight the regions of devices (red), metal interconnect lines (green), and metal I/O pads (black). (B) Bright-field image of mesh nanoelectronics loaded into a glass needle (inner diameter = 95 μm). (C) Bright-field image showing partially ejected mesh nanoelectronics through a glass needle, exhibiting significant expansion and unfolding of the mesh. (D) Semiautomated instrumentation for controlled injection of mesh nanoelectronics, highlighting the motorized translation stage for needle withdrawal (upper orange) and the camera for visualizing the mesh during injection (lower orange). (E) Micro-CT image showing two fully extended mesh nanoelectronics structures (green arrows) inside a mouse brain following controlled injection. Reproduced with permission from refs 13 and 18. Copyright 2015 Nature Publishing Group and American Chemical Society.

mesh nanoelectronics for brain implantation are similar to that discussed above with the additional neural tissue-like/syringe injection constraints of (i) mesh element widths that are no bigger than somata, mechanical flexibility similar to brain tissue and capable of rolling-up in syringe needles, and (ii) nanoelectronic devices positioned to target desired brain regions with interconnects sufficiently long so that I/O connections are well outside the skull postinjection (Figure 5A). For example, we have shown that a 2 mm-wide mesh nanoelectronics can be readily loaded into a 95 μm inner diameter glass needle (Figure 5B) and then partially injected into and unrolled in saline solution (Figure 5C).[13] To achieve precise injection and targeting of distinct brain regions, we developed a semiautomated field-of-view injection process that can be adapted to standard rodent (as well as nonhuman primate and human) stereotaxic surgery stages (Figure 5D). Significantly, this method yields ca. 20 μm targeting precision with fully extended mesh morphology as confirmed by microcomputed tomography (micro-CT) (Figure 5E),[18] thereby allowing specific brain regions or layers to be targeted with mesh devices.

The response of brain tissue to conventional flexible thin-film probes (Figure 6A) and implanted ultraflexible mesh nanoelectronics (Figure 6B) has been evaluated by time-dependent immunohistology studies.[19] First, conventional state-of-the-art flexible electronic probes elicit classic immune response with elevated levels of markers for microglia (Iba-1) and astrocytes (GFAP) and suppression of neurons (NeuN) for all times at the probe interface (Figure 6A). In contrast, brain tissue implanted with mesh nanoelectronics exhibited only slight overexpression of Iba-1 and GFAP, as well as no decrease in neuron signals, at the shortest 2 week time point and, importantly, showed that markers for immune response, Iba-1 and GFAP, and neurons and axons, NeuN and Neurofilament, are all essentially the same as natural background level by 4−6 weeks and maintain this natural distribution of cells to at least 1-year at the probe interface (Figure 6B).[14] In addition, these studies have documented the time-dependent penetration of axonal projections and somata into the interior of mesh nanoelectronics such that near natural cell distributions are achieved both internally and externally to the mesh nanoelectronics at longer times; that is, seamless integration with the brain. This seamless integration is important in that it allows studies to be carried out on natural neural tissue versus that with extrinsic damage and, moreover, suggests unique possibilities for stable long-term monitoring and modulation of neural circuitry.

To carry out chronic multiplexed recording and stimulation studies using syringe-implanted mesh nanoelectronics we have implemented two reliable methods for multichannel I/O connection to standard measurement electronics, including automated conductive ink printing[18] and more recently a "plug-and-play" interface.[20] The plug-and-play method (Figure 7A) is particularly attractive because it is a rapid and user-friendly approach that can be readily adopted by nonexperts in the neuroscience community and also can be adapted to protocols necessary for a human surgical environment. This interface approach retains a standard ultraflexible, tissue-like mesh region for implantation in the brain (Figure 7A(i)), and then routes all interconnect lines via a stem region (Figure 7A(ii)) to individually addressed I/O pads with size and pitch matching standard zero insertion force (ZIF) connectors (Figure 7A(iii)), thus allowing "by hand" plug-and-play connection to standard instrument interface boards (Figure 7A(iv)). For example, connection to a printed circuit board with a standard Omnetics connector yields a compact head-stage for acute and chronic multiplexed recording and stimulation studies in freely behaving animals (Figure 7B).

The above results demonstrating precise implantation, seamless tissue integration, and facile instrument interfacing of the mesh nanoelectronics together allow for chronic electrophysiology studies, where the tissue-like mechanical

DOI: 10.1021/acs.accounts.7b00547
Acc. Chem. Res. 2018, 51, 309−318

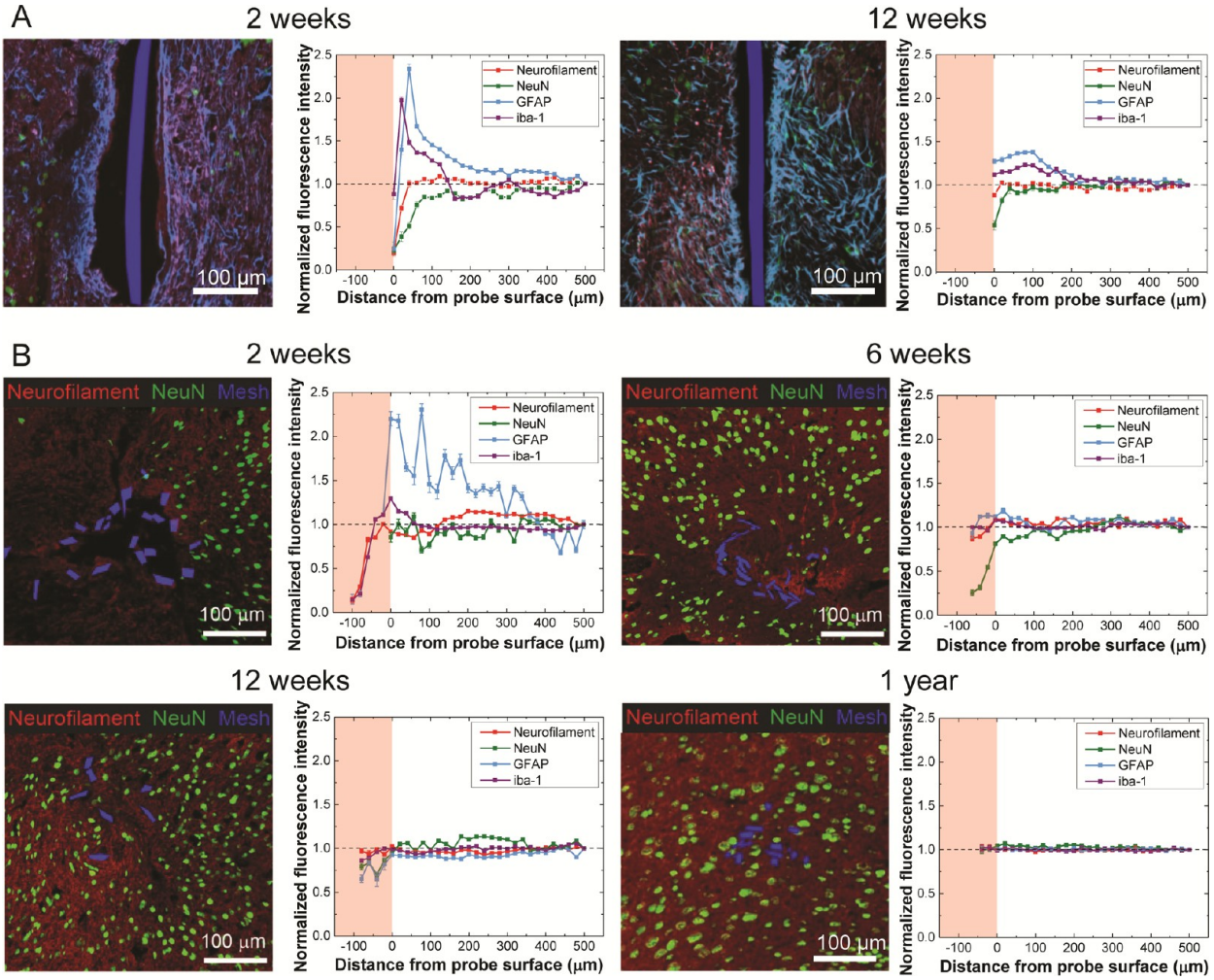

Figure 6. Chronic tissue response of implanted mesh and conventional flexible electronics. Time-dependent immunohistology images of horizontal brain slices containing flexible thin-film probes (A) and mesh nanoelectronics (B) at 2 weeks to 1 year postimplantation. Plots at right of each image display fluorescence intensities versus distance from the probe/brain tissue interface and are normalized against background (black dashed horizontal lines). The pink shaded regions indicate the interior of mesh nanoelectronics. Reproduced with permission from refs 14 and 19. Copyright 2016 Nature Publishing Group and 2017 National Academy of Sciences.

properties and immune response free mesh−tissue interface point to the potential for highly stable chronic measurements. Indeed, we demonstrated single-neuron level recording and stimulation of the same neurons and local circuits on a year time scale in mice,[14] with key results as follows. First, 16-channel multiplexed recordings at 2 and 4 months postinjection showed stable modulation of LFPs and consistent amplitudes of single-unit spikes (Figure 7C). Statistical analyses of recorded single-unit spikes over an 8 month period further revealed stable tracking of the same individual neurons based on consistent principal component analysis (PCA, Figure 7D), similar average spike waveforms (Figure 7E), and largely unchanged interspike interval (ISI) histograms (Figure 7F) and firing rates.[14] In addition, stable phase locking (Figure 7G) for single-neuron firings and theta oscillations in the hippocampus demonstrate the capability to stably monitor the same single neurons and encompassing neural circuits.

Finally, we also incorporated stimulation electrodes into the mesh nanoelectronics as a step toward achieving bidirectional, closed-loop communication with the brain.[14] Simultaneous stimulation and recording at the single-neuron level (Figure 7H) show significantly increased firing rates, which are consistent with stimuli-evoked single-unit responses, in peristimulus spike raster plots. Moreover, first-spike latency histograms following stimulation along with spike sorting and PCA (Figure 7I) show stable single-neuron responses to chronic electrical stimulation over at least a 3-month period.

CONCLUSIONS AND OUTLOOK

The mesh nanoelectronics described in this Account represent a new paradigm for seamless integration of electronics with biological systems. The macroporous mesh with individually addressable nanoelectronic devices is distinct from passive biomaterial scaffolds and conventional flexible electronics and has exceptional compatibilities in terms of chronically stable innervation of synthetic tissues and live animals. With the incorporation of biochemical and electrical sensors, as well as stimulators, in mesh nanoelectronics-innervated tissues, we have demonstrated a 3D electrophysiological mapping and manipulation platform with high temporal resolution to study tissue development, pharmacological responses, and disease mechanisms. Minimally invasive delivery of mesh nanoelectronics with tissue-like structure and mechanical properties into the brains of live rodents has further demonstrated

DOI: 10.1021/acs.accounts.7b00547
Acc. Chem. Res. 2018, 51, 309−318

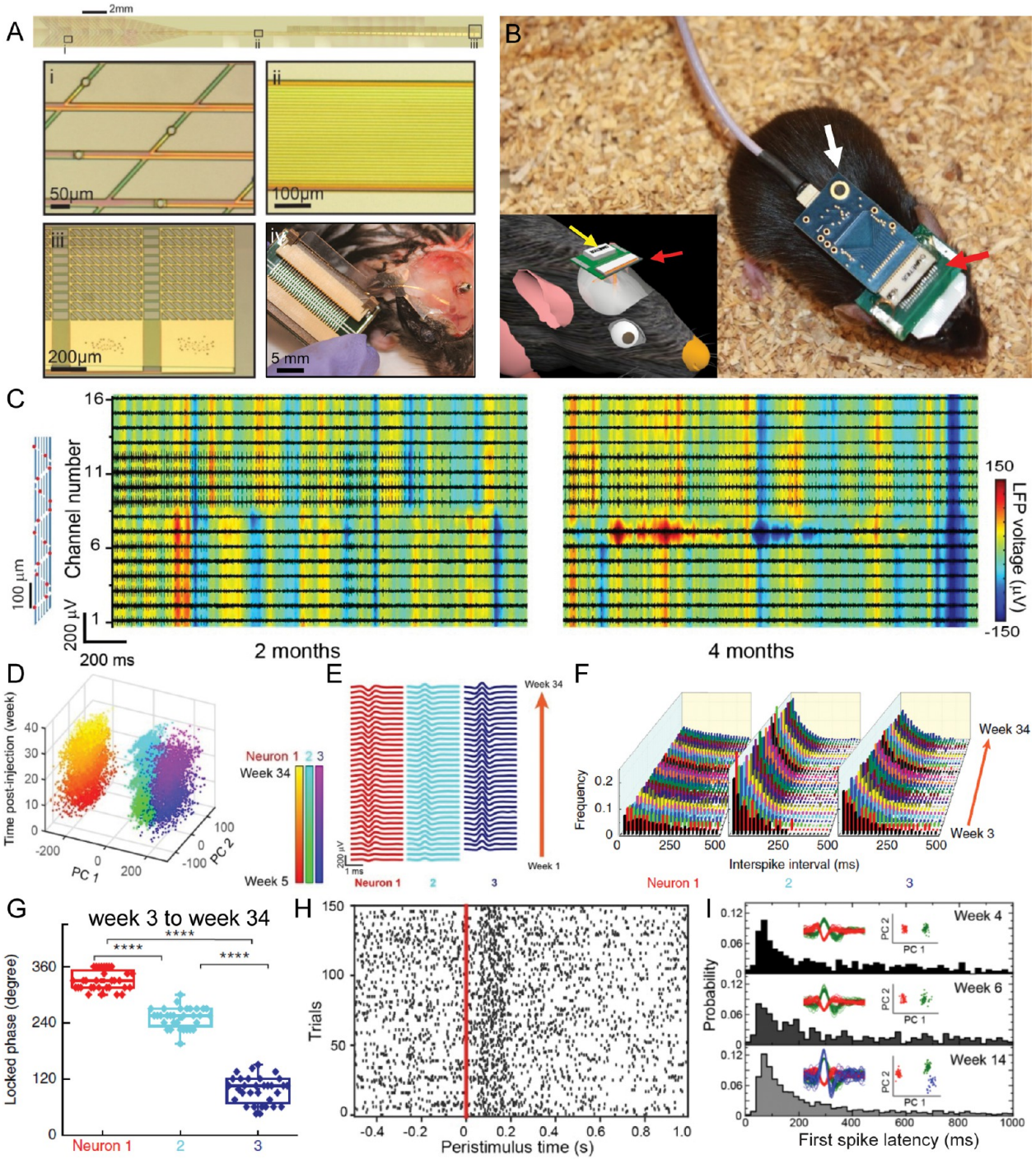

Figure 7. Long-term stable recording and stimulation of brain activity at the single-neuron level with mesh nanoelectronics. (A) Plug-and-play mesh nanoelectronics showing full view (top), enlarged images (bottom, i–iii) and the insertion process (bottom, iv). (B) Photograph of the interface board (red arrow) cemented on the mouse skull forming a compact head-stage (white arrow) for recording from freely behaving animals. Inset, schematic showing electrical connection of 32-channel mesh nanoelectronics to a ZIF connector (red arrow) and a standard Omnetics connector (yellow arrow). (C) 16-channel multiplexed recording of LFP (background heat map) and single-unit firing (foreground black traces) from the same mouse brain at 2 and 4 months postinjection. Leftmost panel, relative positions of the 16 recording electrodes. (D–G) Chronic tracking of the same three neurons by time-dependent PCA (D), averaged spike waveforms (E), ISI histogram (F), and phase locking spike firing rates to theta oscillation (G). (H) Peristimulus raster plot showing spike events (black ticks) of 150 stimulation trials (red solid line, stimulation pulse). (I) First spike latency histograms of stimulus-evoked firings at 4, 6, and 14 weeks postinjection, with insets showing spike sorting (left) and PCA clustering results (right). Reproduced with permission from refs 14 and 20. Copyright 2016 Nature Publishing Group and 2017 American Chemical Society.

successful tracking and modulation of the same neurons and neural circuits on a year time scale, thus providing unprecedented potential for both neuroscience and neurology.

The results obtain with mesh nanoelectronics-innervated synthetic tissues open up rich opportunities for the future (Figure 8) including developing further the capabilities to impact medical treatments. For example, elaboration of the

DOI: 10.1021/acs.accounts.7b00547
Acc. Chem. Res. 2018, 51, 309–318

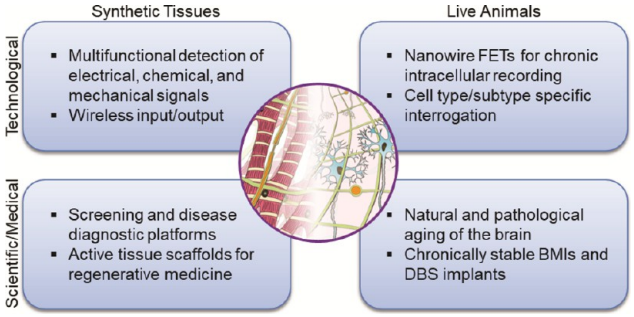

Figure 8. Outlook of mesh nanoelectronics as synthetic tissue scaffolds and *in vivo* probes in nanotechnology, biological sciences, and medicine.

nanosensors for detection of specific biomolecules[6,27] would allow for simultaneous monitoring of biochemical and electrophysiological cellular responses in an innervated synthetic tissue. Looking to the future and the potential for implanted innervated tissue patches, it would also be interesting to explore incorporation of wireless I/O elements. It is also important to recognize that the current paradigm for mesh nanoelectronics-innervated tissue already shows unique capabilities as a platform for pharmacological screening and pathology studies in realistic 3D tissue models. In addition, mesh nanoelectronics can also serve as active tissue scaffolds for regenerative medicine enabling monitoring and control of tissue development in 3D using the individually addressable devices.[12,21]

The mesh nanoelectronics paradigm also opens a myriad of possibilities as *in vivo* brain probes (Figure 8). For example, we believe that pushing the physical limits of mesh nanoelectronics probes by incorporating nanowire FETs[2,6,28] to form synapse-like junctions with neurites can provide unique opportunities for highly localized recording and modulation of LFPs and APs[7,8] and even afford chronic intracellular recording via surface modification to promote cell internalization.[9,29] Similarly, specific functionalization of the ultraflexible mesh nanoelectronics could enable specific cell type or neuron subtype targeting, especially given the absence of an immune response postimplantation.[14,19] The current capabilities of mesh nanoelectronics to record and stimulate single-neuron level activities with long-term chronic stability also can now provide previously unavailable data crucial for understanding important questions in brain science, such as the natural and pathological aging of brain involving long-term physiological changes that must be quantified on the millisecond and micrometer scales of individual neurons.[30] Last, seamless integration of mesh nanoelectronics with the neural tissue over long time periods should make it an ideal platform for brain–machine and deep brain stimulation interfaces where stable single-unit recording would provide unique advances for neuroprosthetic control[31] and closed-loop implants for Parkinsonian patients.[32,33]

AUTHOR INFORMATION

Corresponding Author

*E-mail address: cml@cmliris.harvard.edu.

ORCID

Charles M. Lieber: 0000-0002-6660-2456

Notes

The authors declare no competing financial interest.

Biographies

Xiaochuan Dai received his B.S. in Chemistry from Peking University in 2010 and Ph.D. in Chemistry from Harvard University in 2015, where he is currently a postdoctoral fellow studying nanowire nanoelectronics for integration with synthetic tissues and study of cardiac electrophysiology.

Guosong Hong received his B.S. in Chemistry from Peking University in 2008 and Ph.D. in Chemistry from Stanford University in 2014. He holds a postdoctoral position in the Department of Chemistry and Chemical Biology at Harvard University and is the recipient of a NIH K99 fellowship focused on injectable electronics as a tool to investigate brain aging and cognitive decline.

Teng Gao received his B.S. and Ph.D. in Chemistry from Peking University in 2009 and 2014, respectively. He is a postdoctoral fellow in the Department of Chemistry and Chemical Biology at Harvard University, where his studies focus on developing silicon nanowire based biosensors for point-of-care diagnostic techniques.

Charles M. Lieber is the Joshua and Beth Friedman University Professor at Harvard University, where he holds a joint appointment in the Department of Chemistry and Chemical Biology (as Chair) and Harvard John A. Paulson School of Engineering and Applied Sciences. He received a Ph.D. in Chemistry from Stanford University in 1985 and carried out postdoctoral research at the California Institute of Technology. He joined the faculty of Columbia University in 1987 and moved to Harvard in 1991. His current research focuses on nanoscale materials, nanoelectronics, and neuroscience. He is an elected member of the National Academy of Sciences, National Academy of Medicine and American Academy of Arts and Sciences, and recipient of the MRS Von Hippel Award (2016) and Wolf Prize in Chemistry (2012).

ACKNOWLEDGMENTS

This work is supported by the Air Force Office of Scientific Research (FA9550-14-1-0136), the Naval Research Laboratory (N00173-16-2-C007), a Physical Sciences and Engineering Accelerator award from Harvard University, a Cutting-Edge Basic Research Award from the National Institute on Drug Abuse of the National Institutes of Health (1R21DA043985-01), and a National Institutes of Health Director's Pioneer Award (1DP1EB025835-01). G.H. acknowledges support from an American Heart Association Postdoctoral Fellowship (16POST27250219) and a Pathway to Independence Award from the National Institute on Aging of the National Institutes of Health (1K99AG056636-01).

REFERENCES

(1) Lacour, S. P.; Courtine, G.; Guck, J. Materials and technologies for soft implantable neuroprostheses. *Nat. Rev. Mater.* **2016**, *1*, 16063.

(2) Zhang, A.; Lieber, C. M. Nano-Bioelectronics. *Chem. Rev.* **2016**, *116*, 215–257.

(3) Zhou, W.; Dai, X. C.; Lieber, C. M. Advances in nanowire bioelectronics. *Rep. Prog. Phys.* **2017**, *80*, 016701.

(4) Chen, R.; Canales, A.; Anikeeva, P. Neural recording and modulation technologies. *Nat. Rev. Mater.* **2017**, *2*, 16093.

(5) Polikov, V. S.; Tresco, P. A.; Reichert, W. M. Response of brain tissue to chronically implanted neural electrodes. *J. Neurosci. Methods* **2005**, *148*, 1–18.

(6) Cui, Y.; Wei, Q.; Park, H.; Lieber, C. M. Nanowire nanosensors for highly sensitive and selective detection of biological and chemical species. *Science* **2001**, *293*, 1289–1292.

DOI: 10.1021/acs.accounts.7b00547
Acc. Chem. Res. 2018, 51, 309–318

(7) Patolsky, F.; Timko, B. P.; Yu, G. H.; Fang, Y.; Greytak, A. B.; Zheng, G. F.; Lieber, C. M. Detection, stimulation, and inhibition of neuronal signals with high-density nanowire transistor arrays. *Science* **2006**, *313*, 1100−1104.
(8) Qing, Q.; Pal, S. K.; Tian, B. Z.; Duan, X. J.; Timko, B. P.; Cohen-Karni, T.; Murthy, V. N.; Lieber, C. M. Nanowire transistor arrays for mapping neural circuits in acute brain slices. *Proc. Natl. Acad. Sci. U. S. A.* **2010**, *107*, 1882−1887.
(9) Tian, B. Z.; Cohen-Karni, T.; Qing, Q.; Duan, X. J.; Xie, P.; Lieber, C. M. Three-Dimensional, Flexible Nanoscale Field-Effect Transistors as Localized Bioprobes. *Science* **2010**, *329*, 830−834.
(10) Qing, Q.; Jiang, Z.; Xu, L.; Gao, R.; Mai, L.; Lieber, C. M. Free-standing kinked nanowire transistor probes for targeted intracellular recording in three dimensions. *Nat. Nanotechnol.* **2014**, *9*, 142−147.
(11) Tian, B. Z.; Liu, J.; Dvir, T.; Jin, L. H.; Tsui, J. H.; Qing, Q.; Suo, Z. G.; Langer, R.; Kohane, D. S.; Lieber, C. M. Macroporous nanowire nanoelectronic scaffolds for synthetic tissues. *Nat. Mater.* **2012**, *11*, 986−994.
(12) Dai, X.; Zhou, W.; Gao, T.; Liu, J.; Lieber, C. M. Three-dimensional mapping and regulation of action potential propagation in nanoelectronics-innervated tissues. *Nat. Nanotechnol.* **2016**, *11*, 776−782.
(13) Liu, J.; Fu, T. M.; Cheng, Z.; Hong, G.; Zhou, T.; Jin, L.; Duvvuri, M.; Jiang, Z.; Kruskal, P.; Xie, C.; Suo, Z.; Fang, Y.; Lieber, C. M. Syringe-injectable electronics. *Nat. Nanotechnol.* **2015**, *10*, 629−636.
(14) Fu, T. M.; Hong, G.; Zhou, T.; Schuhmann, T. G.; Viveros, R. D.; Lieber, C. M. Stable long-term chronic brain mapping at the single-neuron level. *Nat. Methods* **2016**, *13*, 875−882.
(15) Xie, C.; Liu, J.; Fu, T. M.; Dai, X. C.; Zhou, W.; Lieber, C. M. Three-dimensional macroporous nanoelectronic networks as minimally invasive brain probes. *Nat. Mater.* **2015**, *14*, 1286−1292.
(16) Yao, J.; Yan, H.; Lieber, C. M. A nanoscale combing technique for the large-scale assembly of highly aligned nanowires. *Nat. Nanotechnol.* **2013**, *8*, 329−335.
(17) Zhao, Y. L.; Yao, J.; Xu, L.; Mankin, M. N.; Zhu, Y. B.; Wu, H. A.; Mai, L. Q.; Zhang, Q. J.; Lieber, C. M. Shape-Controlled Deterministic Assembly of Nanowires. *Nano Lett.* **2016**, *16*, 2644−2650.
(18) Hong, G.; Fu, T. M.; Zhou, T.; Schuhmann, T. G.; Huang, J.; Lieber, C. M. Syringe Injectable Electronics: Precise Targeted Delivery with Quantitative Input/Output Connectivity. *Nano Lett.* **2015**, *15*, 6979−6984.
(19) Zhou, T.; Hong, G.; Fu, T. M.; Yang, X.; Schuhmann, T. G.; Viveros, R. D.; Lieber, C. M. Syringe-injectable mesh electronics integrate seamlessly with minimal chronic immune response in the brain. *Proc. Natl. Acad. Sci. U. S. A.* **2017**, *114*, 5894−5899.
(20) Schuhmann, T. G., Jr.; Yao, J.; Hong, G.; Fu, T. M.; Lieber, C. M. Syringe-Injectable Electronics with a Plug-and-Play Input/Output Interface. *Nano Lett.* **2017**, *17*, 5836−5842.
(21) Feiner, R.; Engel, L.; Fleischer, S.; Malki, M.; Gal, I.; Shapira, A.; Shacham-Diamand, Y.; Dvir, T. Engineered hybrid cardiac patches with multifunctional electronics for online monitoring and regulation of tissue function. *Nat. Mater.* **2016**, *15*, 679−685.
(22) Neri, D.; Supuran, C. T. Interfering with pH regulation in tumours as a therapeutic strategy. *Nat. Rev. Drug Discovery* **2011**, *10*, 767−777.
(23) Kraut, J. A.; Madias, N. E. Metabolic acidosis: pathophysiology, diagnosis and management. *Nat. Rev. Nephrol.* **2010**, *6*, 274−285.
(24) Myles, R. C.; Wang, L. G.; Kang, C. Y.; Bers, D. M.; Ripplinger, C. M. Local beta-Adrenergic Stimulation Overcomes Source-Sink Mismatch to Generate Focal Arrhythmia. *Circ. Res.* **2012**, *110*, 1454−1464.
(25) Hou, J. H.; Kralj, J. M.; Douglass, A. D.; Engert, F.; Cohen, A. E. Simultaneous mapping of membrane voltage and calcium in zebrafish heart in vivo reveals chamber-specific developmental transitions in ionic currents. *Front. Physiol.* **2014**, *5*, 344.
(26) Reynolds, D.; Duray, G. Z.; Omar, R.; Soejima, K.; Neuzil, P.; Zhang, S.; Narasimhan, C.; Steinwender, C.; Brugada, J.; Lloyd, M.; Roberts, P. R.; Sagi, V.; Hummel, J.; Bongiorni, M. G.; Knops, R. E.; Ellis, C. R.; Gornick, C. C.; Bernabei, M. A.; Laager, V.; Stromberg, K.; Williams, E. R.; Hudnall, J. H.; Ritter, P. Micra Transcatheter Pacing Study, G. A Leadless Intracardiac Transcatheter Pacing System. *N. Engl. J. Med.* **2016**, *374*, 533−541.
(27) Zheng, G.; Patolsky, F.; Cui, Y.; Wang, W. U.; Lieber, C. M. Multiplexed electrical detection of cancer markers with nanowire sensor arrays. *Nat. Biotechnol.* **2005**, *23*, 1294−1301.
(28) Zhou, W.; Dai, X.; Fu, T.-M.; Xie, C.; Liu, J.; Lieber, C. M. Long Term Stability of Nanowire Nanoelectronics in Physiological Environments. *Nano Lett.* **2014**, *14*, 1614−1619.
(29) Lee, J. H.; Zhang, A. Q.; You, S. S.; Lieber, C. M. Spontaneous Internalization of Cell Penetrating Peptide-Modified Nanowires into Primary Neurons. *Nano Lett.* **2016**, *16*, 1509−1513.
(30) Morrison, J. H.; Baxter, M. G. The ageing cortical synapse: hallmarks and implications for cognitive decline. *Nat. Rev. Neurosci.* **2012**, *13*, 240−250.
(31) Aflalo, T.; Kellis, S.; Klaes, C.; Lee, B.; Shi, Y.; Pejsa, K.; Shanfield, K.; Hayes-Jackson, S.; Aisen, M.; Heck, C.; Liu, C.; Andersen, R. A. Decoding motor imagery from the posterior parietal cortex of a tetraplegic human. *Science* **2015**, *348*, 906−910.
(32) Kringelbach, M. L.; Jenkinson, N.; Owen, S. L. F.; Aziz, T. Z. Translational principles of deep brain stimulation. *Nat. Rev. Neurosci.* **2007**, *8*, 623−635.
(33) Ashkan, K.; Rogers, P.; Bergman, H.; Ughratdar, I. Insights into the mechanisms of deep brain stimulation. *Nat. Rev. Neurol.* **2017**, *13*, 548−554.

DOI: 10.1021/acs.accounts.7b00547
Acc. Chem. Res. 2018, 51, 309−318